

# Test and Parameters Design of a Novel Reinforced Cymene-Si-Oil Isolator for Reinforcement Scheme of Flimsy Equipment System in Moving Conveyances

Ping Yang<sup>1,\*</sup> - Yong Liu<sup>2</sup> - Fuyun Liu<sup>2</sup>

<sup>1</sup> Jiangsu University, School of Mechanical Engineering, China.

<sup>2</sup> Guilin University of Electronic Technology, Department of Electronic Machinery, China

*The aim of this paper is to provide a systematic investigation of a reinforced isolator for the protection of flimsy electronic equipments system in harsh vibration environment. A Cymene-Si-oil damping isolator is designed and manufactured through coupling the oil and spring by sophisticated methods. The physical mechanism of the actual isolator is investigated. The results of a prototype in dynamic test show complex nonlinear dynamic characteristics. Based on the test, a nonlinear dynamic model for the isolator is presented by analyzing the internal fluid dynamic phenomenon with respect to the isolator. Comparisons with experimental data confirm the validity of the model. In the meantime, an optimal model for parameters matching design is built based on an approximate solution. Finally, the performances of the applying product are described.*

© 2009 Journal of Mechanical Engineering. All rights reserved.

**Keywords:** isolator, damping isolator, dynamic characteristics, mathematical model

## 0 INTRODUCTION

The electronic equipment system is always manufactured as a super-precision system. However, it will be used in harsh environment. For example, the computer in moving conveyances will be activated by vibrations, so it must be reinforced in actual applying processing. Research on the design of isolators to improve the dynamic characteristics of electronic information equipment in moving conveyances has rapidly increased in recent years. Most designs include a vibration isolator to attenuate vibrations so as to improve vibration safety. An accurate characterization of the isolator is of paramount importance for sufficiently precise mathematical models of the isolator for design purposes [1] to [20]. For example, Yang discussed the performance and response of a shock absorber or vibration isolator with combined Coulomb damping, viscous damping quadratic damping and Duffing spring in humorous or random vibration excitations from a theoretical and experimental aspect [1] to [3]. Veprik and Babitsky discussed protection of sensitive electronic equipment from harsh harmonic vibration [4]. Raindra and Mallik discussed the response of the vibration isolator with combined Coulomb damping, viscous damping and hard

Duffing spring [5]. Atanackovic and Spasic discussed viscoelastic compliant contact-impact models [6], while Chandra, et al. discussed the response of the dissipative isolator with combined viscous damping, cubic damping and Duffing spring [7]. Wen, et al. discussed the onset of degenerate hopf bifurcation of a vibro-impact oscillator [8].

The objective of this paper is to provide a systematic investigation of the dynamics or parameters matching design for the protection of the electronic equipment system in a harsh vibration environment (e.g., the computer system in moving conveyances). A micro-structure oil damping isolator is designed through coupling the oil and spring by ingenious tactics according to theoretical studies [1] to [3]. In fact, the damping forces of the isolator show complex nonlinear characteristics in dynamic test. On the basis of the geometric construction and a physical construction of a specific isolator, adopting different degrees of simplification regarding fluid-dynamic phenomena, a mathematical model was developed in this paper to describe the nonlinear phenomena occurring within the isolator. The results obtained by numerical simulation are then compared with the experimental results in order to get an effectiveness rating for the model. To achieve the

---

\*Corr. Author's Address: School of Mechanical Engineering, Jiangsu University, Zhenjiang, 212013, P. R. China, yangpingdm@ujs.edu.cn

optimal design of the isolator, a model is integrated by introducing normalization measure in progress. The approximate formulae are deduced by introducing ingenious transformation-tactics. These approximate theoretical calculating formulae include output response of the system, absolute acceleration transmissibility in vibration etc. So an optimal model for parameters matching design is built for attenuating vibrations of electronic equipment systems. The parameters matching design are developed by computer measure based on the optimal model in progress.

## 1 DESCRIPTION OF REINFORCEMENT FOR ELECTRONIC EQUIPMENTS SYSTEM

Fig. 1 shows a system scheme of the reinforcement system for the electronic equipment system in a moving vehicle. The isolator can be fixed on the base or other sides of a packaging board if there are some vibrations applied in each direction because of the road conditions. In general, the straight direction vibrations and impact is the leading vibrations direction. It must be considered chiefly in reinforcement design for the system. In fact, the reinforcement design is the most economic measure if applying the general electronic equipment to work in a harsh environment. In Fig. 1, the isolator is the key factor for the dynamics of the reinforcement system, therefore, the dynamics of the isolator must be designed in details.

## 2 DESCRIPTION OF PHYSICAL STRUCTURE AND MECHANICAL MODEL OF THE MICRO-CYMENE-Si-OIL COUPLED ISOLATOR

Fig. 2 shows a cross-section of the novel oil damping isolator and its mechanical model. A damping-pot structure is designed to achieve oil-damping function. It can constitute circulating oil chamber with an inner tube and an outer tube (the outer tube is served by the side-department of the crust). There are some orifices on the upside and downside of the inner tube (damping - pot). The oil will flow in a circulating state and dissipate energy by extrusion of the piston reciprocating motion for external vibration excitation. The aim of the isolator is for attenuating vibration by

coupling the oil damping and spring characteristics.

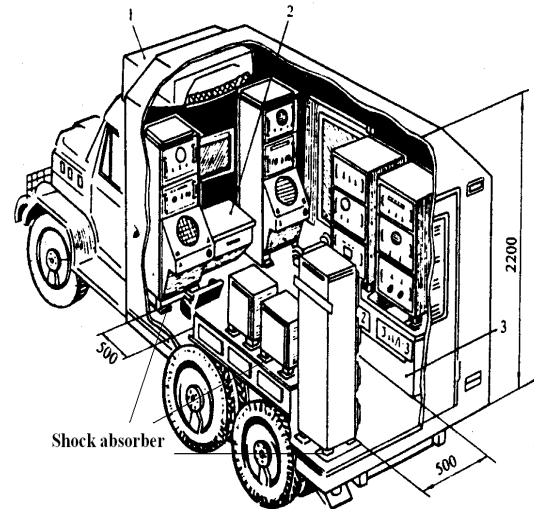


Fig. 1. Physical structure of the reinforcement system for an electronic equipment system

## 3 EXPERIMENTAL RESULTS OF THE WORKING CHARACTERISTICS OF THE ISOLATOR

### 3.1 Experimental Set-Up

The performance of the new type of isolator can be tested by this system. The isolator is mounted on an electrodynamic shaker; the lower end is fixed to the vibrating table of the shaker and the opposite end to the mass block. The signal producer and the power amplifier in Fig. 3 are used to control the shaker, while the time histories of input state variables and output state variables are acquired by means of two accelerometer sensors and an acquisition system (a two-channel data collecting instrument). The electrograph is used to observe the natural state of the signal.

Large amounts of experimental data have been gathered regarding the isolator filled with hydraulic oil. The influence of amplitude and frequency of sine excitation, as well as the influence of fluid viscosity, ratio of damping area was investigated.

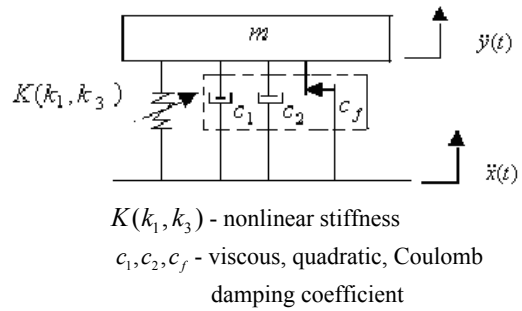
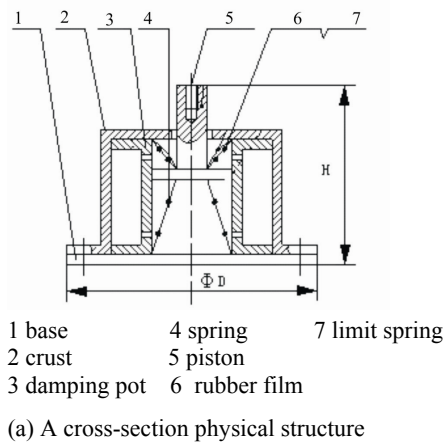


Fig. 2. Physical Structure and Mechanical model of the prototype

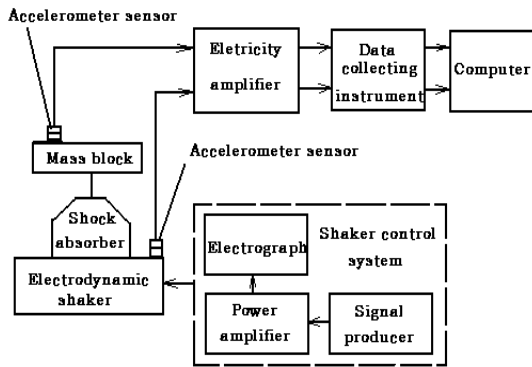


Fig. 3. Experimental Set-Up for Dynamic Testing

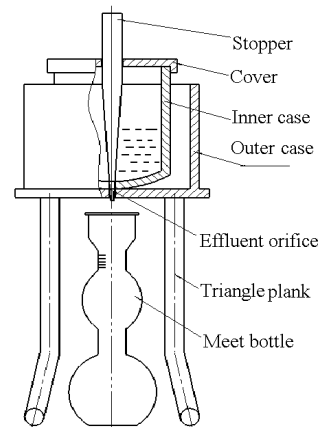


Fig. 4. Experimental set-up for  $(cH)_3SiO[Si(cH_3)_2O]_n Si(cH_3)_3$  viscosity

### 3.2 The Test of Viscosity of Cymene-Si-oil $(cH)_3SiO[Si(cH_3)_2O]_n Si(cH_3)_3$

The cymene-Si-oil was used as damping material in the new isolator. The distinct viscosity of cymene-Si-oil was confected for test using Engler viscometer, the demarcating method was set up (Fig. 4) it is constructed by an Engler viscometer and a precision digital stopwatch meter. The procedure is described:

$$r = \frac{T_1}{T_2} (\approx 52s) \tag{1a}$$

$$v = 7.31r - \frac{6.31}{r} \tag{1b}$$

$$v = 7.31 \frac{T_1}{T_2} - \frac{6.31T_2}{T_1} \tag{1c}$$

where  $r$  is Engler viscosity,  $v$  is kinematic viscosity,  $T_1$  is the outflow time that 200 ml prepared cymene-Si-oil from the viscometer to the meet bottle at some air temperature,  $T_2$  is the outflow time that 200 ml distilled water from the viscometer to the meet bottle at same air temperature.

### 3.3 Experimental Results

One of the basic assumptions made in this study is that the isolator behaves as a Single – Degree of Freedom (SDOF) system. Under this assumption, and since one end of the isolator is held fixed to the shaker and an external time-varying displacement  $x(t)$  or acceleration  $\ddot{x}(t)$  is applied to the this end , the equation of motion of

the free end is given by Newton' second law,

$$m \ddot{y}(t) + f(z, \dot{z}) + \alpha_1 \cdot z(t) + \alpha_3 \cdot z^3(t) = 0, \quad (2a)$$

where  $m$  is the mass which fixed to the another end of the isolator (it represents the mass of equipment),  $\alpha_1, \alpha_3$  is the nonlinear coefficient of the spring, and  $f(z, \dot{z})$  is the coupling damping force of the shock absorber. Based on the above equation we get,

$$f(z, \dot{z}) = -m \ddot{y}(t) - \alpha_1 \cdot z(t) - \alpha_3 \cdot z^3(t) \quad (2b)$$

Because  $z(t) = y(t) - x(t)$  we get,

$$f(z, \dot{z}) = -m(\ddot{y}(t) - \ddot{x}(t)) - \alpha_1 [y(t) - x(t)] - \alpha_3 [y(t) - x(t)]^3. \quad (2c)$$

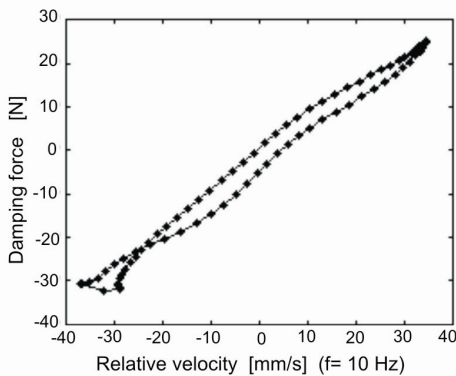
In the experimental setup, we can test the data of  $\ddot{y}(t), \ddot{x}(t)$ . They are the input and output data in the experimental set-up. Therefore, we can get the coupling damping force by applying the equation (2c).

Figs. 5 and 6 illustrate some of the measured damping forces. The curves are presented as damping force versus relative velocity and relative displacement to clearly show the effect of the sine excitation. Comparing Figs. 5 and 6 shows that the nonlinear effect changed as the excitation frequency increased with the higher frequency giving lower output force at the maximum velocity point.

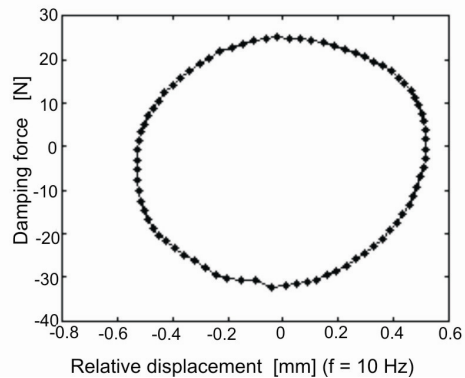
#### 4 MATHEMATICAL MODEL AND NUMERICAL SIMULATION

##### 4.1 Oil Damping

During the isolator motion, the oil flow through the orifices varies with time, not only in value but also in sign. The various damping effects of the hydraulic oil were included in the model.

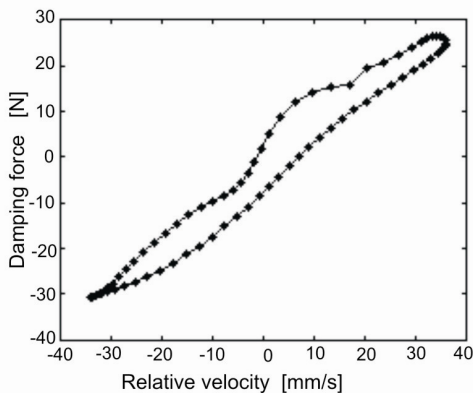


(a) Coupling damping force –relative velocity

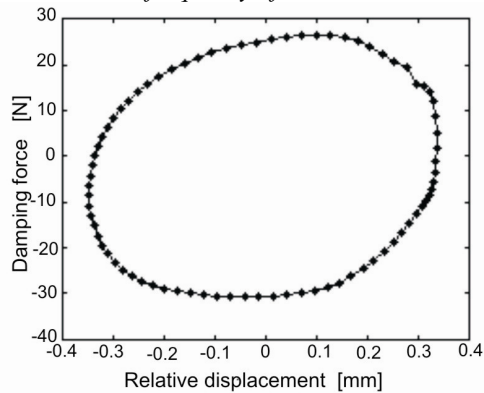


(b) Coupling damping force –relative displacement

Fig. 5. Damping force variations sine excitation, frequency of 10Hz



(a) Coupling damping force –relative velocity



(b) Coupling damping force –relative displacement

Fig. 6. Damping force variations sine excitation, frequency of 15Hz

Assuming that the oil is incompressible, the oil damping force is given by:

(1) *Throttling damping force along the flow path*  

$$Q = A_g \cdot \dot{z}(t). \quad (3)$$

Laminar flow theory yields Poiseuille's equation, where the pressure drop for the throttling loss can be calculated by

$$Q = C_d \cdot \gamma_1 A_n \cdot \sqrt{\frac{2|\Delta P_1|}{\rho}} \cdot \text{sign}(\Delta P_1). \quad (4)$$

So the throttling damping force along the flow path can be calculated as

$$F_1 = A_g \cdot \Delta P_1 = \frac{\rho \cdot A_g^3 \cdot \dot{z}^2(t)}{2C_d^2 \cdot \gamma_1^2 A_n^2} \cdot \text{sign}(\dot{z}(t)). \quad (5)$$

(2) *Laminar flow damping force along the flow path*

Using the same principle, the pressure drop for the laminar flow losses through the orifices can be calculated as

$$Q = n \cdot \frac{\pi d^4 \cdot \Delta P_2}{128L\rho\nu}. \quad (6)$$

Therefore,

$$\Delta P_2 = 128L\rho\nu \frac{A_g}{n\pi(\gamma_2 d)^4} \cdot \dot{z}(t). \quad (7)$$

So the oil damping force along the flow path due to the laminar flow losses can be calculated as

$$F_2 = A_g \cdot \Delta P_2 = 128L\rho\nu \frac{A_g^2}{n\pi(\gamma_2 d)^4} \cdot \dot{z}(t). \quad (8)$$

(3) *Inertia flow damping force along the flow path*

The pressure drop due to the inertia flow loss can be calculated as

$$\Delta P_3 = L\rho \frac{A_g}{\gamma_1 A_n} \cdot \ddot{z}(t), \quad (9)$$

$$F_3 = A_g \cdot \Delta P_3 = L\rho \frac{A_g^2}{A_n} \cdot \ddot{z}(t). \quad (10)$$

#### 4.2 Friction Damping Force

The friction damping force is given by

$$F_4 = F_f \cdot \text{sign}(\dot{z}(t)). \quad (11)$$

#### 4.3 Mathematical Model

Combining these five forces into a mathematical model of the isolator dynamics gives:

$$m\ddot{z}(t) + \frac{\rho \cdot A_g^3 \cdot \dot{z}^2(t)}{2C_d^2 \cdot \gamma_1^2 A_n^2} \text{sign}(\dot{z}(t)) + 128L\rho\nu \frac{A_g^2}{n\pi(\gamma_2 d)^4} \cdot \dot{z}(t) + L\rho \frac{A_g^2}{\gamma_1 A_n} \cdot \ddot{z}(t) + F_f \cdot \text{sign}(\dot{z}(t)) + \alpha_1 z(t) + \alpha_3 z^3(t) = -m\ddot{x}(t), \quad (12)$$

where:

$$z(t) = y(t) - x(t) \quad \dot{z}(t) = \dot{y}(t) - \dot{x}(t) \\ \ddot{z}(t) = \ddot{y}(t) - \ddot{x}(t).$$

The model contains all the physical parameters of the isolators, so it can be used for isolator design.

#### 4.4 Comparison between the Experimental Results and Simulation

Fig. 7 shown the comparison between the experimental results and simulation at frequency of 10 Hz. The numerical simulation can be obtained by using Eq. (12) in MATLAB  $\ddot{x}(t)$  is the actual input signal.

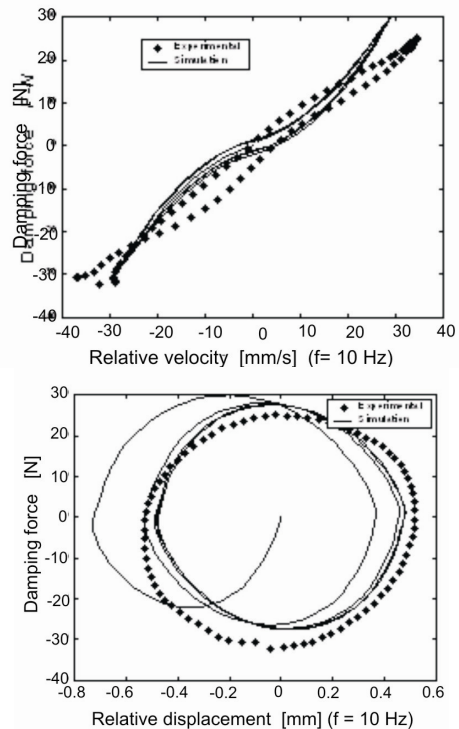


Fig. 7. Comparison between the experimental results and simulation

The numerical simulation can simulate the actual characteristics of the isolator in approximate by contrasting the experimental results and the numerical simulation. There is a light distortion in the simulation results that may be caused without introducing the compressibility of oil or other errors (metrical errors and data managing error).

### 5 THE OPTIMAL MODEL FOR PARAMETERS MATCHING DESIGN OF THE ISOLATOR BASED ON APPROXIMATE SOLUTION

#### 5.1 Approximate Analytical Solution in Vibrations

By considering Fig. 2b and Eq. (12), a well-connected mathematical model can be induced as Eq. (13), assuming that the excitation is the displacement harmonic excitation.

$$m\ddot{z} + c_1\dot{z}|\dot{z}| + c_2\dot{z} + c_f \operatorname{sgn}(\dot{z}) + k_1z + k_3z^3 = ma_0\omega^2 \sin(\omega t), \tag{13}$$

where

$$c_1 = \frac{\rho \cdot A_g^3}{2C_d^2 \cdot \gamma_1^2 A_n^2}$$

$$c_2 = 128L\rho v \frac{A_g^2}{n\pi(\gamma_2 d)^4}$$

$$c_f = F_f \quad k_1 = \alpha_1 \quad k_3 = \alpha_3.$$

Assuming the following non-dimensional parameters:

$$T = \omega_0 t \quad u = \omega / \omega_0 \quad \lambda = z / a_0$$

$$\xi_1 = c_1 a_0 / 2m \quad \xi_2 = c_2 / (2m\omega_0)$$

$$\omega_0 = \sqrt{k_1 / m}$$

$$\xi_f = c_f / (2ma_0\omega_0^2) \quad \varepsilon_2 = k_2 a_0^2 / (m\omega_0^2) = k_2 a_0^2 / k_1$$

$$\dot{\lambda} = \dot{z} / (a_0\omega_0) \quad \ddot{\lambda} = \ddot{z} / (a_0\omega_0^2).$$

Substituting them into an Eq. (13) yields:

$$\ddot{\lambda} + 2\xi_1\dot{\lambda}|\dot{\lambda}| + 2\xi_2\dot{\lambda} + 2\xi_f \operatorname{sgn}(\dot{\lambda}) + \lambda + \varepsilon_2\lambda^3 = u^2 \sin(uT), \tag{14}$$

where  $\dot{\lambda}$ ,  $\ddot{\lambda}$  denote differentiation with respect to non-dimensional time  $T$ .

Assuming the solution is:

$$\lambda = \lambda_0 \sin(uT + \varphi).$$

We get:

$$\dot{\lambda} = \lambda_0 u \cos(uT + \varphi), \quad \ddot{\lambda} = -\lambda_0 u^2 \sin(uT + \varphi).$$

The sign function can be approximated by Fourier expansion up to first order as

$$f_1 = \operatorname{sgn}[\sin(\omega t + \varphi)] \approx r_{01} + r_{11} \cos(\omega t + \varphi) +$$

$$r_{21} \sin(\omega t + \varphi) \approx \frac{4}{\pi} \sin(\omega t + \varphi),$$

where:

$$r_{01} = \frac{1}{T'} \int_0^{T'} \operatorname{sgn}[\sin(\omega t + \varphi)] dt = 0,$$

$$r_{11} = \frac{2}{T'} \int_0^{T'} \operatorname{sgn}[\sin(\omega t + \varphi)] \cos \omega t dt = 0,$$

$$r_{21} = \frac{2}{T'} \int_0^{T'} \operatorname{sgn}[\sin(\omega t + \varphi)] \sin \omega t dt = \frac{4}{\pi}.$$

$$f_2 = \operatorname{sgn}[\cos(\omega t + \varphi)] \approx r_{02} + r_{12} \cos(\omega t + \varphi) +$$

$$r_{22} \sin(\omega t + \varphi) \approx \frac{4}{\pi} \cos(\omega t + \varphi),$$

where:

$$r_{02} = \frac{1}{T'} \int_0^{T'} \operatorname{sgn}[\cos(\omega t + \varphi)] dt = 0,$$

$$r_{12} = \frac{2}{T'} \int_0^{T'} \operatorname{sgn}[\cos(\omega t + \varphi)] \cos \omega t dt = \frac{4}{\pi},$$

$$r_{21} = \frac{2}{T'} \int_0^{T'} \operatorname{sgn}[\cos(\omega t + \varphi)] \sin \omega t dt = 0,$$

$$\text{where } T' = \frac{2\pi}{\omega}.$$

Substituting them into Eq. (14) yields

$$-\lambda_0 u^2 \sin(uT + \varphi) + 2\xi_1 \lambda_0^2 u^2 \cos^2(uT + \varphi) \operatorname{sgn}(\dot{\lambda}) + 2\xi_2 \lambda_0 u \cos(uT + \varphi) + 2\xi_f \operatorname{sgn}(\dot{\lambda}) + \lambda_0 \sin(uT + \varphi) + \varepsilon_2 \lambda_0^3 \sin^3(uT + \varphi) = u^2 \sin uT, \tag{15}$$

$$2\xi_f \operatorname{sgn}(\dot{\lambda}) + \lambda_0 \sin(uT + \varphi) +$$

$$\varepsilon_2 \lambda_0^3 \sin^3(uT + \varphi) = u^2 \sin uT,$$

or

$$-\lambda_0 u^2 \sin(uT + \varphi) +$$

$$2\xi_1 \lambda_0^2 u^2 \left[ \frac{1}{2} + \frac{1}{2} \cos 2(uT + \varphi) \right] \operatorname{sgn}(\dot{\lambda}) +$$

$$2\xi_2 \lambda_0 u \cos(uT + \varphi)$$

$$+ 2\xi_f \operatorname{sgn}(\dot{\lambda}) + \lambda_0 \sin(uT + \varphi) + \tag{16}$$

$$\varepsilon_2 \lambda_0^3 \left[ \frac{3}{4} \sin(uT + \varphi) - \frac{1}{4} \sin 3(uT + \varphi) \right]$$

$$= u^2 [\sin(uT + \varphi) \cos \varphi - \cos(uT + \varphi) \sin \varphi].$$

Equating coefficients of the same harmonics and the constant terms from both sides of the equations, the following is obtained:

$$-\lambda_0 u^2 + \lambda_0 + \frac{3}{4} \varepsilon_2 \lambda_0^3 = u^2 \cos \varphi, \tag{17}$$

$$\frac{4}{\pi} \xi_1 \lambda_0^2 u^2 + 2 \xi_2 \lambda_0 u + \frac{8}{\pi} \xi_f = -u^2 \sin \varphi. \quad (18)$$

Eliminating  $\varphi$  from Eq. (17) and (18), we get:

$$\left[ \frac{4}{\pi} \xi_1 \lambda_0^2 u^2 + 2 \xi_2 \lambda_0 u + \frac{8}{\pi} \xi_f \right]^2 + \quad (19)$$

$$[-\lambda_0 u^2 + \lambda_0 + \frac{3}{4} \varepsilon_2 \lambda_0^3]^2 = u^4,$$

$$\varphi = -\arctg \frac{\frac{4}{\pi} \xi_1 \lambda_0^2 u^2 + 2 \xi_2 \lambda_0 u + \frac{8}{\pi} \xi_f}{-\lambda_0 u^2 + \lambda_0 + \frac{3}{4} \varepsilon_2 \lambda_0^3}. \quad (20)$$

The absolute acceleration transmissibility is defined as the ratio of maximum acceleration of the mass block to that of the base motion. It can be shown that

$$\begin{aligned} T_f &= \left| \frac{(\ddot{z} + \ddot{x})_{\max}}{\ddot{x}_{\max}} \right| = \left| \frac{(\ddot{z} - a_0 \omega^2 \sin \omega t)_{\max}}{a_0 \omega^2} \right| \\ &= \left| \frac{(a_0 \omega_0^2 \ddot{\lambda} - a_0 \omega^2 \sin \omega t)_{\max}}{a_0 \omega^2} \right| \\ &= |(-\lambda_0 \sin(\omega t + \varphi) - \sin \omega t)_{\max}| \\ &= \sqrt{1 + \lambda_0^2 + 2 \lambda_0 \cos \varphi}. \end{aligned} \quad (21)$$

### 5.2 The Optimal Model for Parameters Matching Design of the Isolator

The optimal model is built based on the above.

Design variables:

$$X = [\xi_1 \ \xi_2 \ \xi_3 \ k_1 \ k_3]. \quad (22)$$

Dual objective function:

$$T_f = \sqrt{1 + \lambda_0^2 + 2 \lambda_0 \cos \varphi} \longrightarrow \min. \quad (23)$$

The constraints:

For vibration

$$\left[ \frac{4}{\pi} \xi_1 \lambda_0^2 u^2 + 2 \xi_2 \lambda_0 u + \frac{8}{\pi} \xi_f \right]^2 + \quad (24)$$

$$[-\lambda_0 u^2 + \lambda_0 + \frac{3}{4} \varepsilon_2 \lambda_0^3]^2 = u^4.$$

By considering the physical condition based on the structure and material property, we must give the limit of the various damping and stiffness.

$$\xi_{1x} \leq \xi_1 \leq \xi_{1s} \quad (25)$$

$$\xi_{2x} \leq \xi_2 \leq \xi_{2s} \quad (26)$$

$$\xi_{fx} \leq \xi_f \leq \xi_{fs} \quad (27)$$

$$k_{10} \leq k_1 \leq k_{1H} \quad (28)$$

$$k_{30} \leq k_3 \leq k_{3H}.$$

(29)

The computer program can be developed for the optimal design by this model.

### 5.3 Example for Engineering Design

An electronic information equipment will work in a moving vehicle environment. The mass of the equipment is 12 kg. The isolators will be designed for the protection of the information equipment. The technology demands are:

- (1) The amplitude of sine excitation on base is equal to 5 mm.
- (2) The allowable value of absolute acceleration transmissibility in vibration must be less than 1.5.

#### Solution for algorithm:

Three isolators can be selected. The natural frequency of the isolator must be designed in 8 to 12 Hz for obtaining an isolator that has a broad isolation and enough stiffness. Then the computer program can be designed by applying the Eqs. (22) to (29), the results are:

$$\xi_1 = 0.28 \quad \xi_2 = 0.15 \quad \xi_f = 0.4$$

$$k_1 = 8500 \text{ N/m} \quad k_3 = -7.2 \cdot 10^8 \text{ N/m}^3$$

$$T_f = 1 \text{ (no resonance peak)}.$$

The mentioned parameters can be changed as the physical parameters. Good performance can be achieved by an experimental test based on actual isolator. The technology indexes are:

- (1) The rated load is equal to 4 kg.
- (2) The value of the absolute acceleration transmissibility on the resonance point in vibration is close to 1.
- (3) The optimal structure dimension is close to the 60 to 70% of the evaluating design structure dimensions by experience. The contrast between some classic isolator and our products can be shown in Table 1.

## 6 CONCLUSIONS

- (1) A novel reinforced Cymene-Si-Oil isolator was designed for the reinforcement scheme of the flimsy equipment system in moving conveyances. It has a good dynamic

performance and controllable design-capability (see Table 1).

Table 1. *The contrast between some products*

Contrast project	Steel wire isolator USA	No-peak isolator China	Isolator (Our product)
Type (rated load)	SCS (3 to 5 kg)	GWF-5 (3 to 5 kg)	sample (3 to 5 kg)
$F$	8 to 9 Hz	5 Hz	8 to 12 Hz
$T_f$	< 3 ( $\leq 2$ )	1	< 2
Isolating efficiency	< 70 %	$\leq 1$	> 70 Hz > 82%

- (2) A mathematical model for simulating dynamic behavior of the isolator has been developed in order to describe the characteristics occurring within the isolator. The numerical simulation has showed that the model can the actual isolator.
- (3) An optimum model for the parameters matching selection of the isolator is built. The design example is illustrated to confirm the validity of the modeling method and the theoretical solution.

### 7 NOMENCLATURE

- $Q$  the oil flowrate between the two oil chambers  
 $A_g$  average area of piston by considering the rod  
 $C_d$  dynamic discharge coefficient (oil)  
 $\rho$  hydraulic oil density  
 $d$  diameter of the oil orifice  
 $A_n$  orifice area (oil)  
 $\nu$  kinematic viscosity  
 $L$  length of the oil orifice  
 $F_f$  estimation of the friction of the system  
 $n$  number of orifice  
 $\alpha_1$  linear stiffness coefficient of the spring  
 $\alpha_3$  cubic stiffness coefficient of the spring  
 $\Delta P$  pressure difference  
 $\gamma_1$  correspond coefficient of the area of the orifice when circumfluence  
 $\gamma_2$  correspond coefficient of the diameter of the orifice when circumfluence  
 $\omega_0$  natural frequency of the isolator  
 $\omega$  excitation frequency  
 $a_0$  amplitude of excitation acting on the base  
 $c_1$  quadratic damping coefficient  
 $c_2$  viscous damping coefficient  
 $c_f$  Columb damping force  
 $k_3$  cubic stiffness coefficient  
 $k_1$  linear-stiffness coefficient

- $T_f$  absolute acceleration transmissibility in vibration  
 $z(t)$  relative displacement between mass block and base  
 $x(t)$  displacement excitation on base  
 $\ddot{z}$  relative acceleration between mass block and base  
 $y(t)$  output displacement on mass block  $\dot{z}$  relative velocity between mass block and base  
 $\ddot{x}$  acceleration excitation on base  
 $\ddot{y}$  output acceleration on mass block  
 $r_{01}, r_{11}, r_{21}$  the first order Fourier expanding coefficient of the sign function  
 $f_1 = \text{sgn}[\sin(\omega t + \varphi)]$   
 $r_{02}, r_{12}, r_{22}$  the first order Fourier expanding coefficient of the sign function  
 $f_2 = \text{sgn}[\cos(\omega t + \varphi)]$

### 8 ACKNOWLEDGMENTS

The authors would like to acknowledge the support of National Natural Science Foundation of China, National Defense Natural Science Foundation of China, International cooperative Project of Jiangsu Province, Special Science Foundation for Doctoral Unit of China, the support of Natural Science Foundation of Gangxi province of China, and Natural Science Foundation for Qualified Personnel of Jiangsu University during the course of this work.

### 9 REFERENCES

- [1] Yang, P. (2001) Research on design, modelling, simulation and testing of nonlinear coupling shock absorber. Ph.D Dissertation. Huazhong university of science and technology. (In Chinese)
- [2] Yang, P. (2005), Numerical characteristics of multi-medium coupling vibration isolator. J.



- of Mechanical Engineering, vol. 56, no. 5, p. 289-305.
- [3] Yang, P., Tan Yonghong, Yang Jiangming, *etal* (2006), Measurement, simulation on dynamic characteristics of a wire gauze-fluid damping shock absorber. *Mechanical systems and signal processing*, vol. 20, no. 3, p. 745-756.
- [4] Veprik, A.M., Babitsky, V.I., (2000), Vibration protection of sensitive electronic equipment from harsh harmonic vibration, *Journal Sound and Vibration*, vol. 238, no. 1, p. 19-30.
- [5] Raindra, B., Mallik, A.K. (1993) Hard duffing-type vibration isolator with combined coulomb and viscous damping. *Int. J. Non-linear Mchanics*, vol. 28, no. 4, p. 427-440.
- [6] Atanackovic, T.M, Spasic, D.T. (2004), On viscoelastic compliant contact-impact models. *Transactions of the ASME. Journal of Applied Mechanics*, vol. 71, no. 1, p. 134-142.
- [7] Chandra, N., Shekhar, H. Hatwal (1998), Response of non-linear dissipative shock isolators. *J. of Sound and Vibration*. vol. 214, no. 4, p. 589-603.
- [8] Wen, GuiLin, Xie, Jianhua and Xu, Daolin (2004) Onset of degenerate hopf bifurcation of a vibro-impact oscillator. *Journal of Applied Mechanics, Transactions ASME*, vol. 71, no. 4, p. 579-581.
- [9] Sheng Jingchao, (1980) *Hydraulic Fluid Mechanics*. Beijing: Machine Press. (In Chinese)
- [10] Audenino, A.L., Belingardi, G. (1995) Modelling the dynamic behavior of motorcycle damper. *Proc Instn. Mech. Engrs. Part D: J. of Automobile Engineering*, 209, p. 249-262.
- [11] Surace, C., Worden, K., Tomlinson, G. (1992) On the non-linear characteristics of automotive shock absorbers. *Proc Instn. Mech.Engrs. Part D: J. of Automobile Engineering*, 206, p.3-16.
- [12] Wallascbek, J. (1990) Dynamics of nonlinear automotive shock absorbers. *Int. J. Non-linear Mechanics*, 25, 299-308.
- [13] Harris, C.M., Crede, C.E. (1990) *Shock and Vibration Handbook*. MC-Graw-Hill.
- [14] Evkin, A. (2004) Symptotic investigation of vehicle isolator with reversing shell of revolution. *International Journal of Vehicle Design*, vol. 34, no. 4, p. 399-410.
- [15] Reciprocating seal for shock absorber applications. *Sealing Technology*, no. 7, July, 2004, p. 10.
- [16] Holdhusen, M.H., Cunefare, K.A. (2004) Optimization of a state-switched absorber applied to a continuous vibrating system. *Proceedings of the SPIE - The International Society for Optical Engineering*, vol. 5386, no. 1, p. 319-28
- [17] Yang. P. (2003) Experimental and mathematical evaluation of dynamic behaviour of an oil-air coupling shock absorber. *Mechanical Systems and Signal Processing*, vol. 17, no. 6, p. 1367-1379.
- [18] Yang. P., Liao Ningbo, Yang Jianbo (2008) Design, Test and modeling evaluation approach of a Novel Si-Oil shock absorber for protection of electronic equipment in moving vehicles. *Mechanism and Machine Theory*, vol. 43, no. 1, p. 18-32.
- [19] Yang. P. (2006) Approximate solution of a multi-medium coupling nonlinear isolator under random vibration excitation, *Gongcheng Lixue/Engineering Mechanics*, vol. 23, no. 7, p. 170-175. (In Chinese)
- [20] Yang. P. (2007) Numerical analysis for dynamic transmissibility of a mixed nonlinear shock absorber. *Communications in numerical methods in engineering*, vol. 23, no. 12, p. 1121-1130.